GEOPHYSICAL RESEARCH LETTERS, VOL. 23, NO. 3, PAGES 225-228, FEBRUARY 1, 1996

Neutrally buoyant diapirs: A model for Venus coronae

Dorothy M. Koch[1]
Department of Geology and Geophysics, Yale University, New Haven, Connecticut

Michael Manga[2]
Department of Geology and Geophysics, University of California, Berkeley

Abstract. Coronae are typically circular features, 100-600 km in diameter, characterized by a deformed annular ring that is often topographically high. The central region may be raised or depressed relative to the ambient elevation. Previous studies have proposed an evolutionary progression beginning with dome-shaped features which have radiating extensional rifts, followed by plateau-shaped features which have both concentric deformation and radial extension, ending with the classic corona as described above. Previous dynamical calculations of a rising and spreading diapir simulated the evolution from dome to plateau-shaped topography, but could not account for the raised rim or depressed central topography of some coronae. We demonstrate that these features can be modeled by a diapir that spreads laterally at a depth of neutral buoyancy.

Introduction

Coronae are among the features of Venus that indicate a planetary history different from the Earth's. They often appear in chains or clusters, and the associated volcanism is reminiscent of terrestrial volcanic chains. However the mechanism and planetary structure responsible for their unusual shapes remain unknown. Planetary surface features such as the crustal and lithospheric thicknesses [e.g. *Simons et al.*, 1994], the thermal gradient, and the elastic properties near the surface are poorly constrained. Of greater certainty are the observations that there is very little lateral motion of the surface [e.g. *Solomon et al.*, 1992; *Grimm* 1994], that the surface is hot (≈740 K), basaltic in composition and appears to be dry [*Kaula*, 1990], and that plume activity and volcanism are prominent.

We propose a mechanism for the formation of corona topography that is consistent with the more certain aspects of venusian surface structure, and can help inform the less certain aspects. As in several previous studies [*Stofan et al.*, 1991; *Stofan et al.*, 1992; *Squyres et al.*, 1992; *Janes et al.*, 1992], we envision corona formation to result from ascending, buoyant mantle plumes or diapiric upwellings. Close to the surface, they spread laterally, generating partial melts that may erupt at the surface. *Koch* [1994] modeled the ascent and spread of a diapir beneath a free-slip fluid surface and found that the induced surface topography evolves from a dome to a plateau. Here we demonstrate that a diapir spreading at a level of neutral buoyancy produces additional topographic features characteristic of coronae. The level of neutral buoyancy may occur within the lithosphere, between the mantle and crust [*Hansen & Phillips* 1993], or along the gabbro-eclogite phase transition.

Model

The model problem (figure 1) consists of an initially spherical diapir with radius a, density ρ and viscosity $\lambda\mu$ rising through a fluid half-space having density ρ_m, and spreading laterally at a depth b, beneath a layer having ρ_c, such that $\rho_m > \rho > \rho_c$.

We assume cylindrical geometry, Newtonian fluids, and a Boussinesq-like approximation. The diapir motion and topography are solved numerically using a boundary integral method [*Manga et al.*, 1993; *Koch* 1994]. The upper surface has a free-slip boundary condition, and dynamic topography is calculated using the surface viscous stress. We assume uniform viscosity μ for the upper and lower layers. Since diapirs are hot and much less viscous than the surrounding lithosphere, we assume $\lambda = 0.01$. The effects of plume cooling are ignored, since the time scale of cooling for a plume having dimension $l \approx 100$ km is $O(l^2/\kappa) \approx 300$ m.y. (where $\kappa \approx 10^{-6}$ m^2/s is thermal diffusivity) and is much larger than the time scale of diapiric evolution, ≈ 50 m.y. (see below). We also assume that the deflection of the interface between the upper and lower layers is negligible. The portion of the diapir which has penetrated b is negatively buoyant, and the portion of the diapir beneath b is positively buoyant.

Solutions to the model problem depend on the dimensionless depth of neutral buoyancy, b/a, and the density structure

$$\Gamma = (\rho - \rho_c)/(\rho_m - \rho_c). \quad (1)$$

We present results for $\Gamma = 0.8$, a value suitable for a diapir spreading at a gabbro-eclogite phase transition. A slightly higher value of Γ might apply for spreading

[1]Now at Columbia University/GISS, New York, New York.
[2]Now at Department of Geological Sciences, University of Oregon, Eugene, Oregon.

Paper number 95GL03776
0094-8534/96/95GL-03776$03.00

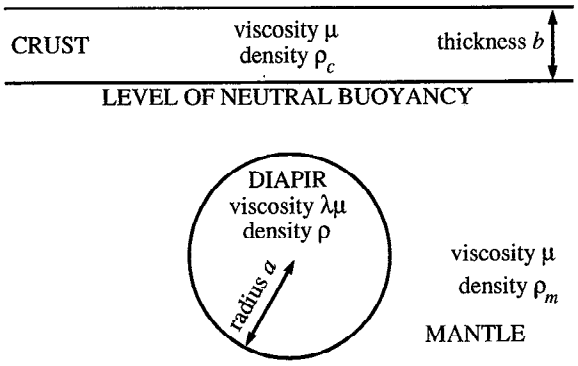

Figure 1. Model geometry. Initial diapir depth is $10a$.

along the crust-mantle interface. We consider $0.05 < b/a < 0.5$, consistent with the large range of possible diapiric radii and crustal thickness.

Model results

In figure 2 we show computed diapir shapes and the corresponding surface topography at four times for $b/a = 0.1$ and $\Gamma = 0.8$. Figure 3 shows the surface deviatoric stress for the earliest and latest stages shown in figure 2. Also shown are the surface deformations which would result if the deviatoric stress magnitude is great enough to fracture the surface crustal material. Domal topography and radial fractures result from early diapir ascent. As the diapir spreads along the level of neutral buoyancy, rims and concentric deformation develop. The concentric deformation becomes increasingly focused close to the rim as spreading continues. At late stages, the central region becomes depressed below the surrounding surface. The topographic evolution is explained by the change in buoyancy of the diapir above and below b. At early stages the diapir is nearly spherical, and even when its upper surface has first penetrated b, the net buoyancy is dominated by the lower portion of the diapir, resulting in domal topography. As the diapir flattens and thins, its central region has protruded furthest through b and contributes a greater amount of negative buoyancy than the outer region of the diapir which has still barely penetrated b. Hence the central region of the surface subsides faster than the outer region and a rim forms. For sufficiently large Γ and/or b/a, the negative force is great enough to generate a central depression.

Early stages resemble the observed domal features with radial fractures, sometimes termed 'novae'. Intermediate features resemble typical coronae. Finally, a central depression evolves, generating a feature like those which have previously been termed 'calderas' (assumed to have central collapsed magma chambers) [*Squyres et al.* 1992; *Stofan et al.* 1992]. However these depressions may be a late stage of corona formation. The evolution from the dome to the corona with a cen-

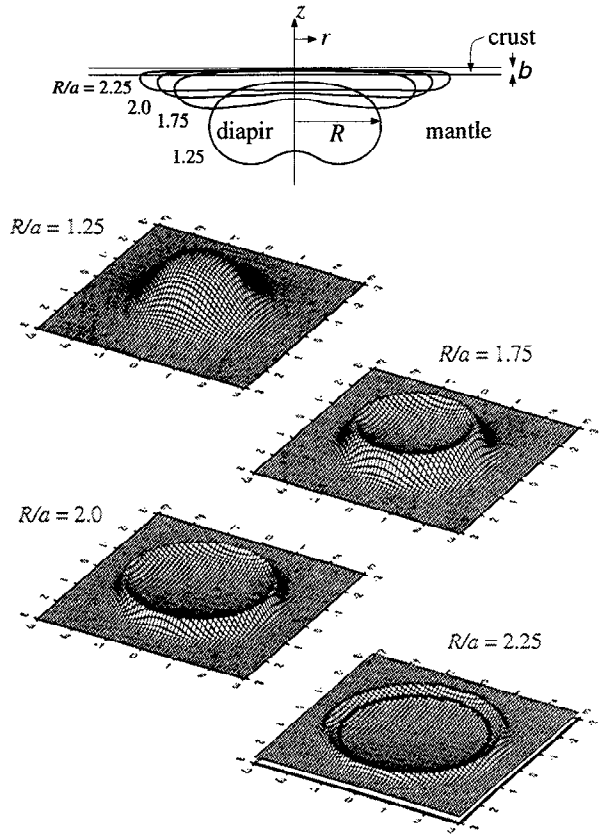

Figure 2. Diapir shapes and model topography at $R/a = 1.25$, 1.75, 2.0 and 2.25 for $b/a = 0.1$ and $\Gamma = 0.8$. Times are normalized by $\mu/(\rho_m - \rho)ga$, and $t = 0$ is defined to occur when $R/a = 1.25$. Topography is normalized by $a(\rho_m - \rho)/\rho_c$. Plots are vertically exaggerated by a factor of 6.

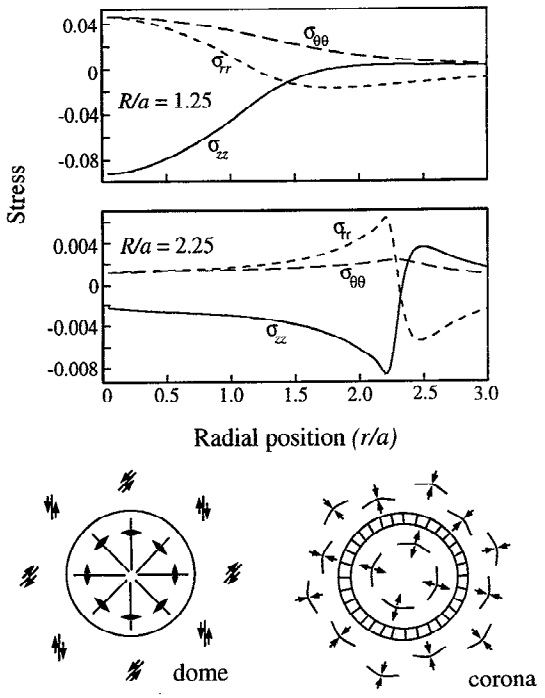

Figure 3. The dimensionless viscous deviatoric surface stresses for $R/a = 1.25$ and $R/a = 2.25$, corresponding to the first and last stages in figure 2. Stress is normalized by $ag(\rho_m - \rho)$. Bottom: The corresponding expected patterns of deformation.

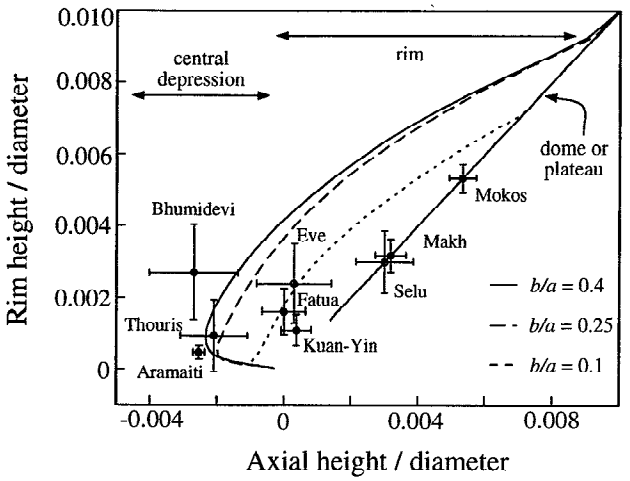

Figure 4. Rim elevation as a function of axial height for $\Gamma = 0.8$ and $b/a = 0.4$, 0.25 and 0.1. Both elevations are divided by diapir diameter. The model results are dimensionalized using $a(\rho_m - \rho)/\rho_c$, where $\rho = 2.9$, 3.3 and 3.4 for the crust, diapir and mantle. Also shown are observations for several coronae, normalized by corona diameter. The error bars reflect spatial topography variations.

tral depression takes ≈ 50 m.y., assuming $\mu = 10^{21}$ Pas, $a = 100$ km, and $\rho_m - \rho = 100$ kg/m^3.

In general, large values of b/a produce the greatest topographic relief at early times and then deeper central depressions, whereas low values of b/a produce nearly plateau-shaped topography. For very large b/a (e.g. $b/a > 0.4$) the diapir remains too deep to produce significant relief. Γ affects the topography in a similar manner: greater relief occurs for larger values of Γ.

Comparison with observations

The evolution of the rim and axial elevation is illustrated in figure 4, for three model values of b/a, and is compared with several corona observations. We normalize the calculated rim and axial heights by the diapir diameter, and observations by the coronae diameter ($\approx$ the diapir diameter). A given corona shape begins in the center of the diagram and evolves along the straight line (containing the domal features Selu, Makh and Mokos) toward the upper right hand corner, while the topography has a dome or plateau shape. Once a rim forms, it then progresses counterclockwise along one of the curves with the appropriate value of b/a.

The solution for each corona could be inverted to obtain b and a. Figure 4 indicates the appropriate value of b/a and the amount of diapiric spreading for each corona. The value of a can then be found by requiring the solution to match the diameter of the corona. However this inversion is not attempted here.

In figure 5 we show that two different coronae can be modeled by a diapir spreading at a depth of neutral buoyancy of $b = 20$ km. Typically we find good agreement with observations for $0.7 < \Gamma < 0.95$ and 10 km $< b <$ 50 km.

Discussion

A variety of coronae shapes and sizes can be explained by diapirs spreading along a depth where they are neutrally buoyant. This depth might be the mantle-crust boundary, or alternatively the gabbro-eclogite phase transition. For the phase transition, Γ is 0.8, assuming $\rho \approx 2.9$, 3.4, and 3.3 g/cm^3 for gabbro, eclogite and the diapir respectively. Although we have assumed that the lower fluid is a halfspace, rather than a finite eclogite layer, the part of the plume that would extend beneath the eclogite layer is unlikely to affect significantly the surface features. Diapiric spreading along such a phase boundary may also promote the detachment of the eclogite layer, which in turn would affect the dynamic topography and the spreading of the diapir. For spreading along the mantle-crust interface, a slightly larger value of Γ is appropriate. In this case, if the diapir's buoyancy is due to thermal expansion, $\Gamma \approx 0.9$ ($\rho_m - \rho \approx 50$ kg/m^3 for a temperature anomaly of several hundred degrees; $\rho_m - \rho$ could be even larger due to compositional buoyancy or if the diapir is partially molten). The larger value of Γ will produce slightly greater topographic relief and deeper central depressions.

We have assumed that the interface between the layers is not deflected by the approach and penetration of the diapir. Such deflection would warp the entire profile upward, but the corona features would still be produced. We have also assumed a free-slip upper surface, which is an end-member of possible rheological models. The existence of an elastic lid, suggested by both observational and theoretical constraints [e.g. *Johnson & Sandwell* 1994], might suppress some of the short-wavelength dynamical features such as the rims. How-

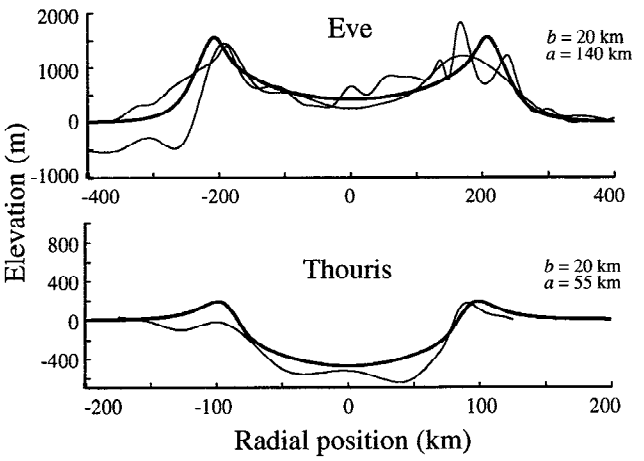

Figure 5. Comparison of model profiles (bold curves) with observed profiles (thin curves). Top: Eve corona, compared with the solution for $b = 20$ km and $a = 140$ km at $R/a = 1.74$. Bottom: Thouris corona (thought previously to be a caldera), compared with the solution for $b = 20$ km and $a = 55$ km at $R/a = 1.54$. For both cases, $\Gamma = 0.8$. Model results are dimensionalized using $a(\rho_m - \rho)/\rho_c$.

ever, for viscoelastic properties, the Maxwell time for the lithosphere is unlikely to be greater than $O(10^6)$ years, whereas the diapir spreads over a timescale $O(10^7-10^8)$ years. We therefore expect surface deformation to be dominated by the viscous response. We have also neglected vertical viscosity gradients within the lithosphere. However, previous studies have demonstrated that the presence of a high viscosity lid (as opposed to an elastic lid) would actually enhance the amplitude of short wavelength features such as the rims [e.g. *Morgan* 1965].

The model fails to reproduce the topographic troughs which surround many of the coronae annular rims. These might be explained by gravitational compensation due to the topographic loading of the corona [*Squyres et al.*, 1992], or by thermal effects such as cooling of the nose of the spreading diapir.

One variation of the model (not presented here) is to place the depth of neutral buoyancy within a fluid having a smoothly, e.g. exponentially, varying density structure. Such a structure would also be appropriate for neutrally buoyant magma bodies as discussed by *Head & Wilson* [1992]. Rim-shaped topography still occurs, but the topographic features are less sharp and relief is lower.

The simple model of neutrally buoyant diapirs can account for many of the previously unsolved aspects of corona topography. In particular, rim-shaped topography with high central topography occurs at early stages and sunken central topography at later stages. We have found that many coronae shapes can be reproduced for different values of crustal thickness, within a range 10 km $< b <$ 50 km for the density structure $\Gamma = 0.8$ (equation 1). A careful comparison of model results and coronae observations can provide improved constraints on the density structure and crustal thickness on Venus.

Acknowledgments. We thank H.A. Stone for assistance with the integral equation formulation. D. Bindschadler, D. Jurdy, J. DeLaughter and two anonymous reviewers are thanked for suggestions and comments. M. Manga is supported by the Miller Institute for Basic Research in Science.

References

Grimm, R.E., Recent deformation rates on Venus, *J. Geophys. Res.*, *99*, 23,163-23,171, 1994.

Hansen, V.L. & R.J. Phillips, Tectonics and volcanism of Eastern Aphrodite Terra, Venus: No subduction, no spreading, *Science*, *260*, 526-530, 1993.

Head, J.W. & L. Wilson, Magma reservoirs and neutral buoyancy zones on Venus: Implications for the formation and evolution of volcanic landforms, *J. Geophys. Res.*, *97*, 3877-3903, 1992.

Janes, D.M., S.W. Squyres, D.L. Bindschadler, G. Baer, G. Schubert, V.L. Sharpton & E.R. Stofan, Geophysical models for the formation and evolution of coronae on Venus, *J. Geophys. Res.*, *97*, 16,055-16,068, 1992.

Johnson C.L. & D.T. Sandwell, Lithospheric flexure on Venus, *Geophys. J. Int.*, *119*, 627-649, 1994.

Kaula, W.M., Venus: A contrast in evolution to Earth, *Science*, *247*, 1191-1196, 1990.

Koch, D.M., A spreading drop model for plumes on Venus, *J. Geophys. Res.*, *99*, 2035-2052, 1994.

Manga, M., H.A. Stone & R.J. O'Connell, The interaction of plume heads with compositional discontinuities in the Earth's mantle, *J. Geophys. Res.*, *98*, 19,979-19,990, 1993.

Morgan, W.J., Gravity anomalies and convection currents. 1. A sphere and cylinder sinking beneath the surface of a viscous fluid, *J. Geophys. Res.*, *70*, 6175-6187, 1965.

Simons, M., B.H. Hager & S.C. Solomon, Global variations in the geoid/topography admittance of Venus, *Science*, *264*, 798-803, 1994.

Solomon, S.C. et al., Venus tectonics: An overview of Magellan observations, *J. Geophys. Res.*, *97*, 13,199-13,256, 1992.

Squyres, S.W., D.M. Janes, G. Baer, D.L. Bindschadler, G. Schubert, V.L. Sharpton & E.R. Stofan, The morphology and evolution of coronae on Venus, *J. Geophys. Res.*, *97*, 13,611-13,634, 1992.

Stofan, E.R., D.L. Bindschadler, J.W. Head & E.M. Parmentier, Corona structures on Venus: Models of origin, *J. Geophys. Res.*, *96*, 20,933-20,946, 1991.

Stofan, E.R., V.L. Sharpton, G. Schubert, G. Baer, D.L. Bindschadler, D.M. Janes & S.W. Squyres, Global distribution and characteristics of coronae and related features on Venus: Implications for origin and relation to mantle processes, *J. Geophys. Res.*, *97*, 13,347-13,378, 1992.

Dorothy M. Koch, Columbia University/GISS, 2880 Broadway, New York, NY 10025

Michael Manga, Department of Geological Sciences, University of Oregon, Eugene, OR 97403

(received March 17, 1995;
revised July 5, 1995;
accepted November 12, 1995.)